Int. J. Heat Mass Transfer. Vol. 32, No. 11, pp. 2155–2166, 1989
Printed in Great Britain

0017–9310/89 $3.00+0.00

Stability of lid-driven shallow cavity heated from below

A. A. MOHAMAD and R. VISKANTA
School of Mechanical Engineering, Purdue University, West Lafayette, IN 47907, U.S.A.

(*Received* 31 *January* 1989 *and in final form* 6 *April* 1989)

Abstract—Hydrodynamic and thermal stability of combined thermal buoyancy and lid-driven shear flow in a shallow cavity is analyzed by means of linearized perturbation theory. The analysis considers a cavity heated from below and cooled at the upper moving lid. A numerical procedure, which has generality with respect to boundary conditions, Reynolds, and Prandtl numbers, is described for solution of the linearized model equations. A direct numerical integration (Runge–Kutta with Newton–Raphson) method is used to solve the differential conservation equations. This method gives an exact result for the classical Benard problem where the flow becomes unstable at a critical Rayleigh number, $Ra_c = 1707.76$. The numerical results show the existence of two critical wave numbers depending on whether the dominant force driving the flow is due to buoyancy or shear. For $Pr \leqslant 0.1$ the instability is due to the buoyancy force for constant heat flux boundary conditions, while for $Pr = 1$ the instability is due to the shear force. Increasing the Reynolds number stabilizes the flow, and reducing the Prandtl number makes the flow more unstable.

INTRODUCTION

IT IS WELL known that a fluid in a rectangular cavity heated from below is unstable when the Rayleigh number exceeds a critical value for which the viscous force can no longer support the buoyancy force. Therefore, the equilibrium cannot be maintained within the fluid giving rise to the formation of convective cells. At higher temperature differences the stationary roll patterns become unstable and a time-dependent flow develops [1]. This problem, known as the Benard problem, continues to challenge researchers [2–5]. The stability of stratified channel flows has been considered by many researchers studying the onset of vortices in fully developed laminar channel flow heated from below [6–12]. Chandra [6] appears to have been the first one to perform experiments on the effect of shear force (Couette flow) on the Benard problem. Gallagher and Mercer [7] solved linear stability equations for plane Couette flow with the heated lower plate. Their analysis was limited to $Re \leqslant 150$ (where Re is based on the half distance between the plates), and the predictions were compared with the experimental data of Chandra [6].

Di Prima and Stuart [13] and Bayly *et al.* [14] reviewed the theoretical and experimental developments on stability and transition in plane Poiseuille and Couette flows for isothermal conditions, and Platten and Legros [15] considered stability under a variety of circumstances, including channel, natural, and mixed convection flows. Experimental results show [15] that the transverse rolls are preferred over the longitudinal rolls in the developing regions of Poiseuille flow and that for small rates of shear the transverse rolls are formed at the boundary of the plane Couette flow [6]. However, no experimental and theoretical results for a closed cavity heated from below in the presence of shear appear to have been reported, and the stability of mixed (thermal and shear driven) convection has not been studied. This may be due to the range of Reynolds numbers considered, because such a transition from thermal to shear driven flow is clearly evident at higher Reynolds numbers. It is recognized that shear does not change the critical Rayleigh number for longitudinal rolls in Benard convection but influences the stability of other modes. The focus in the paper is on other modes, because the solution of Benard's problem is already available [1]. The stability of flow in shallow cavities driven by combined shear and buoyancy forces is relevant to industrial processes such as coating, galvanizing and glass manufacturing by the float process [16] as well as to geophysical [17, 18] problems. In float glass production, for example, a glass ribbon moves over molten tin contained in a bath, and the instability of flow affects the quality of the product.

This paper considers the hydrodynamic and thermal stability in a shallow cavity where flow is induced by a buoyancy force due to bottom heating combined with a shear force resulting from the motion of the upper lid of the cavity. In most cases the linear stability analysis provides valuable information about the mechanism of the instability. The results of linear stability analysis are often used as a starting point of a non-linear analysis, and this has provided the motivation for the present work. The Prandtl number effects were studied and the results show a marked variation in the stability mechanism of the flow, depending upon the magnitude of the Reynolds and Prandtl numbers and the imposed thermal boundary conditions.

NOMENCLATURE

Bi_1 Biot number at the lower boundary of the cavity, $h_1 H/k$
Bi_2 Biot number at the upper boundary of the cavity, $h_2 H/k$
g gravitational acceleration
H height of cavity, see Fig. 1
h_1 heat transfer coefficient at the lower boundary
h_2 heat transfer coefficient at the upper boundary
l length of cavity, see Fig. 1
k thermal conductivity of the fluid
k_1 wave number in the x-direction
k_2 wave number in the y-direction
p pressure
Pe Peclet number, $Re\,Pr$
Pr Prandtl number, ν/α
Ra Rayleigh number, $g\beta(T_1-T_2)H^3/\nu\alpha$
Re Reynolds number, $U_0 H/\nu$
$\hat{Re}$ wave number Reynolds number, $(Re\,k_1)/\alpha$
T temperature
t time
U_0 velocity of the moving upper plate
$\bar{u}$ dimensionless mean velocity, u/U_0
x horizontal coordinate, see Fig. 1
z vertical coordinate, see Fig. 1.

Greek symbols
α thermal diffusivity or $(k_1^2+k_2^2)^{1/2}$
β thermal expansion coefficient
η_i dimensionless coordinate, x_i/H
θ dimensionless temperature, $(T-T_2)/(T_1-T_2)$
ξ dimensionless coordinate, z/H
ρ density
σ complex growth rate
τ dimensionless time, $t\nu/H^2$.

Subscripts
c critical value
i x, y or z velocity component or imaginary component
1 lower horizontal plate at $z=0$
2 moving upper horizontal plate at $z=H$.

Superscripts
′ perturbation quantity
¯ mean quantity.

STABILITY ANALYSIS

The physical model and the coordinate system of the problem considered are shown in Fig. 1. The bottom is heated and maintained at a higher temperature than the upper lid, which moves at a constant velocity. Robin boundary conditions (convective boundary conditions) are considered in the modeling. This type of boundary conditions is more general and realistic than constant heat flux or constant temperature boundary conditions. The cavity is considered to be shallow, $L/H \gg 1$. For the problem considered the Boussinesq approximation permits the conservation equations of mass, momentum, and energy to be written as [15]

$$\frac{\partial u_i}{\partial x_i}=0 \tag{1}$$

$$\frac{\partial u_i}{\partial t}+u_j\frac{\partial u_i}{\partial x_j}=-\frac{1}{\rho}\frac{\partial p}{\partial x_i}+\nu\frac{\partial^2 u_i}{\partial x_j\partial x_j}+g\beta(T-T_2)\lambda_i \tag{2}$$

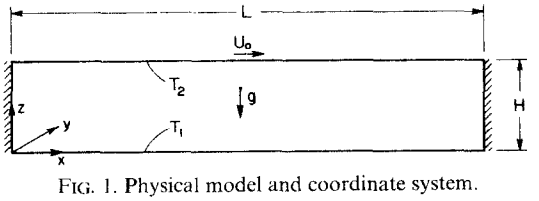

FIG. 1. Physical model and coordinate system.

$$\frac{\partial\theta}{\partial t}+u_j\frac{\partial\theta}{\partial x_j}=\alpha\frac{\partial^2\theta}{\partial x_j\partial x_j} \tag{3}$$

where λ_i is a unit vector in the direction of the buoyancy force. Non-parallel flow exists only in the end regions. The basic flow is considered to be parallel and end effects are neglected.

For steady, laminar parallel flow [i.e. $u(z)$, $v=w=0$] the continuity, momentum, and energy equations can be written as

$$\int_0^H u\,dz=0 \tag{4}$$

$$0=-\frac{1}{\rho}\frac{\partial p}{\partial x}+\nu\frac{\partial^2 u}{\partial z^2} \tag{5}$$

$$0=-\frac{1}{\rho}\frac{\partial p}{\partial z}+g\beta(T-T_2) \tag{6}$$

$$0=\frac{\partial^2 T}{\partial z^2}. \tag{7}$$

The boundary conditions are

$$u=0 \quad \text{and} \quad T=T_1 \quad \text{at} \quad z=0$$
$$u=U_0 \quad \text{and} \quad T=T_2 \quad \text{at} \quad z=H. \tag{8}$$

The solution of the above equations after normalizing z, u, T with H, U_0 and T_1-T_2, respectively, yields

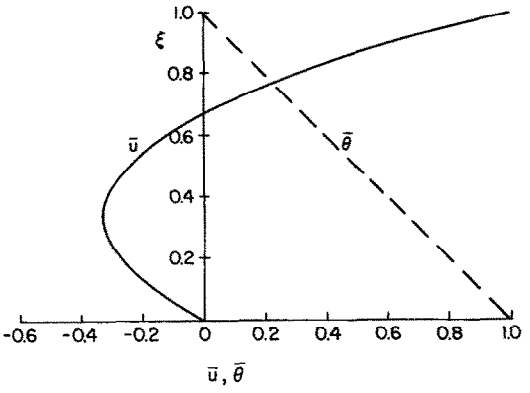

FIG. 2. Core velocity and temperature distributions.

$$\bar{u} = -3\xi(1-\xi)+\xi \tag{9}$$

$$\bar{\theta} = 1-\xi. \tag{10}$$

The velocity and temperature profiles in the core region are shown in Fig. 2.

The stability of the flow can be analyzed by introducing a small disturbance in the flow: $u = \bar{u}+u'$; $v = v'$; $w = w'$; $p = \bar{p}+p'$ and $\theta = \bar{\theta}+\theta'$ where the primed quantities are perturbed variables and the bars denote the steady-state flow velocity components, pressure and temperature. Using H^2/ν, H, α/H and (T_1-T_2) for scaling time, length, perturbed velocities, temperature (the lid velocity is used to scale the steady velocity), and introducing the perturbed quantities into the conservation equations while neglecting the products of small quantities, the conservation equations become

$$\frac{\partial u_i'}{\partial \eta_i} = 0 \tag{11}$$

$$\frac{\partial u_i'}{\partial \tau}+Re\left(\bar{u}_j\frac{\partial u_i'}{\partial \eta_j}+u_j'\frac{\partial \bar{u}_i}{\partial \eta_j}\right) = -\frac{\partial p'}{\partial \eta_i} + \frac{\partial^2 u_i'}{\partial \eta_j \partial \eta_j}+Ra\,\theta'\lambda_i \tag{12}$$

$$Pr\frac{\partial \theta'}{\partial \tau}+Pe\,\bar{u}_j\frac{\partial \theta'}{\partial \eta_j}+u_j'\frac{\partial \bar{\theta}}{\partial \eta_j} = \frac{\partial^2 \theta'}{\partial \eta_j \partial \eta_j}. \tag{13}$$

The boundary conditions are taken as

$$u' = 0 \quad \text{at} \quad \xi = 0, 1 \tag{14a}$$

$$\mathrm{D}\theta'+Bi_1\,\theta' = 0 \quad \text{at} \quad \xi = 0 \tag{14b}$$

$$\mathrm{D}\theta'+Bi_2\,\theta' = 0 \quad \text{at} \quad \xi = 1 \tag{14c}$$

where $\mathrm{D} = \mathrm{d}/\mathrm{d}\xi$.

Assuming the perturbations have the following form:

$$F(t,x,y,z) = F(z)\,e^{\sigma t+i(k_1x+k_2y)} \tag{15}$$

where $F(z)$ and σ are complex quantities; i.e.

$$F(z) = F_r+iF_i \tag{16}$$

$$\sigma = \sigma_r+i\sigma_i. \tag{17}$$

The substitution of equation (15) into equations (11)–(14) yields

$$ik_1u'+ik_2v'+\mathrm{D}w' = 0 \tag{18}$$

$$\sigma u' = -ik_1P'-Re(ik_1\bar{u}u'+w'\mathrm{D}\bar{u}) +(\mathrm{D}^2-k_1^2-k_2^2)u' \tag{19}$$

$$\sigma v' = -ik_2P'-i\,Re\,\bar{u}k_1v'+(\mathrm{D}^2-k_1^2-k_2^2)v' \tag{20}$$

$$\sigma w' = -\mathrm{D}P'-i\,Re\,\bar{u}k_1w'+(\mathrm{D}^2-k_1^2-k_2^2)w'+Ra\,\theta' \tag{21}$$

$$\sigma\,Pr\,\theta' = -Pe\,\bar{u}k_1\theta'-w'\mathrm{D}\bar{\theta}+(\mathrm{D}^2-k_1^2-k_2^2)\theta'. \tag{22}$$

Setting $k_1 = 0$ in the above equations (longitudinal mode) eliminates the effect of the mean flow (i.e. Reynolds number) on the perturbed quantities v', w' and θ'. The only effect of the Reynolds number is to modify the u' velocity. Solution of equations (20)–(22) with the aid of equation (18) for the longitudinal modes leads to the Benard problem. Results for this problem are available in the literature [1]. By setting $k_2 = 0$ and considering the transverse modes, equations (10)–(22) become

$$ik_1u'+\mathrm{D}w' = 0 \tag{23}$$

$$\sigma u' = -ik_1P'-Re(\bar{u}ik_1u'+w'\mathrm{D}\bar{u})+(\mathrm{D}^2-k_1^2)u' \tag{24}$$

$$\sigma v' = -i\,Re\,\bar{u}k_1v'+(\mathrm{D}^2-k_1^2)v' \tag{25}$$

$$\sigma w' = -\mathrm{D}P'-i\,Re\,\bar{u}k_1w'+(\mathrm{D}^2-k_1^2)w'+Ra\,\theta' \tag{26}$$

$$\sigma\,Pr\,\theta' = -i\,Pe\,\bar{u}k_1\theta'-w'\mathrm{D}\bar{\theta}+(\mathrm{D}^2-k_1^2)\theta'. \tag{27}$$

Eliminating the pressure term from equations (24)–(26) and using equation (23), gives

$$\mathrm{D}^4w' = (\sigma+2k_1^2+ik_1\,Re\,\bar{u})\mathrm{D}^2w' -(\sigma k_1^2+k_1^4+ik_1\,Re\,\mathrm{D}^2\bar{u}+ik_1^3\,Re\,\bar{u})w'+k_1^2\,Ra\,\theta' \tag{28}$$

and

$$\mathrm{D}^2\theta' = (\sigma\,Pr+i\,Pe\,\bar{u}k_1+k_1^2)\theta'+w'\mathrm{D}\bar{\theta}. \tag{29}$$

The boundary conditions are

$$\mathrm{D}w' = w' = 0 \tag{30a}$$

$$\mathrm{D}\theta'+Bi_1\,\theta' = 0 \quad \text{at} \quad \xi = 0 \tag{30b}$$

and

$$\mathrm{D}\theta'+Bi_2\,\theta' = 0 \quad \text{at} \quad \xi = 1. \tag{30c}$$

When Bi_1 and Bi_2 are set to zero, constant heat flux boundary conditions are simulated. If Bi_1 and Bi_2 are set to infinity this corresponds to constant temperature boundary conditions. The model equations are rather complex and no closed form solutions appear possible.

The analysis presented above is directly applicable to situations where k_1 and k_2 are not equal to zero

(oblique wave). Using Squire's theorem [15], assuming that $k_1^2+k_2^2=\alpha^2$ and $k_1 Re=\alpha \widehat{Re}$, and introducing the above definitions into equations (18)–(22), after some algebraic manipulations leads to equations similar to equations (28) and (29). If k_1 is replaced by α and $k_1 Re$ by $\alpha \widehat{Re}$, the Rayleigh numbers are not changed. Therefore, the results based on the above analysis are applicable to $k_1 \neq 0$ and $k_2 \neq 0$.

METHOD OF SOLUTION

Linear ordinary differential equations which arise in stability analyses have been solved by various authors using different techniques such as the Galerkin method [19, 20], local potential method [11], pseudospectral method with Chebyshev series [21] or direct numerical integration [11, 22, 23]. The latter method is straightforward in formulation and superior in accuracy compared to the other methods which depend on the type of basic functions and number of expansion terms. It was chosen for these reasons even though it has some disadvantages. The method is sensitive to the initial guess of the parameters Ra and σ. However, this difficulty can be overcome by scanning the range of wave numbers for given Reynolds and Prandtl numbers. In most cases the initial value of k_1 was taken as 0.05 and increased by 0.1 or 0.05 each iteration, and Ra and σ were set to 2000 and 0, respectively. For example, to scan the value of k_1 from 0.05 to 7 required about 140 data points.

The first step in the solution is to write equations (28)–(30) as a system of first-order equations split into real and imaginary parts by assuming that

$$w_j = v_{2j-1}+iv_{2j} \tag{31}$$

where

$$w_1 = w, \quad w_1 = v_1+iv_2$$
$$w_2 = Dw_1, \quad w_2 = v_3+iv_4, \text{ etc.} \tag{32}$$

In equation (17) $\sigma_r = 0$ corresponds to neutral stability. Equations (28) and (29) are sixth order, but they can be written as a system of six first-order equations. Splitting the resulting equations into real and imaginary parts gives twelve first-order equations.

The solution vector can be expressed as a linear combination of six linearly independent solutions, i.e.

$$w = \sum_{j=1} C_j w^j \tag{33}$$

with initial values

$$w_i^j = \delta_{ij}. \tag{34}$$

From the boundary conditions at $\xi = 0$, equation (30), we have that

$$C_1 = C_2 = 0 \tag{35a}$$

and

$$C_6+Bi_1 C_5 = 0 \tag{35b}$$

and from the second set of boundary conditions at $\xi = 1.0$, equation (3), we have that

$$D_{ct} = \begin{bmatrix} w_1^3(1) & w_1^4(1) & w_1^5(1)-Bi_1 w_1^6(1) \\ w_2^3(1) & w_2^4(1) & w_2^5(1)-Bi_1 w_2^6(1) \\ Bi_2 w_5^3(1)-w_6^3(1) & Bi_2 w_5^4(1)-w_6^4(1) & Bi_2 w_5^5(1)-Bi_1 Bi_2 w_5^6(1)+Bi_1 w_6^6(1)-w_6^5(1) \end{bmatrix}. \tag{36}$$

The three columns of the above determinant are computed by integrating the system of equations (28) and (29) four times. Each integration is performed with different initial conditions, i.e. with $j = 3, 4, 5, 6$ in equation (33), using a standard numerical Runge–Kutta method. The determinant, equation (36), is complex, but its real and imaginary parts should vanish at the critical values of the parameters (Ra and σ_i). In order to determine the critical values of Ra and σ_i that make the determinant vanish a Newton–Raphson method is used to find successively better approximations for Ra and σ_i.

Table 1. Effect of Prandtl and Reynolds numbers on the critical Rayleigh number

Pr	Re	Ra_c Poiseuille	Couette
0.1	100	1742.22	2358.50
	400	2274.38	8743.27
0.01	100	1730.06	2201.65
	400	2030.23	6073.87

RESULTS AND DISCUSSION

The basic velocity distribution, equation (9), is for combined Couette and Poiseuille flow. The first term stands for the Poiseuille flow and the second term for the Couette flow. Isothermal Couette flow is stable for all Reynolds numbers as predicted by the linear stability analysis [24], whereas Poiseuille flow is unstable for a Reynolds number of 5772.2 [25]. Heating of the above flows from below leads to thermal instability. The critical Rayleigh number increases with increasing Reynolds number (Table 1). A simple relationship is predicted for Couette flow between σ_i and k_1, for the neutral stability curve. This relationship is a function of the Reynolds number and independent of the Prandtl number

$$\sigma_i = (Re\, k_1)/2. \tag{37}$$

The wave speed is seen to increase with the Reynolds number. For fixed values of Re, the Poiseuille flow is more unstable than the Couette flow (Table 1).

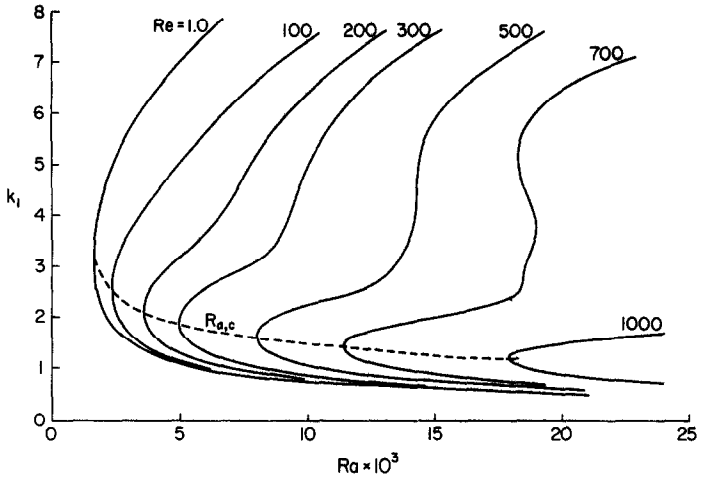

FIG. 3. Variation of wave number with Rayleigh number for different Reynolds numbers, $Pr = 0.01$, constant temperature boundary conditions.

Also, the critical wave number is almost constant for Poiseuille flow ($k_1 = 3.1$).

The more general convective boundary conditions, equations (14b) and (14c), permit examination of two special cases. The limit when $Bi_1 = Bi_2 = \infty$ corresponds to constant temperature boundary conditions, and the limit when $Bi_1 = Bi_2 = 0$ corresponds to the constant heat flux boundary conditions. The results for these two limiting cases are discussed first.

Constant temperature boundary conditions

The computer program was first tested for the Benard problem ($Re = 0$) and for fully developed laminar flow in a parallel-plate channel heated from below. The same results as those reported in the literature [11] were obtained. The program converges very rapidly for small Reynolds and Prandtl numbers. As these parameters are increased the method becomes very sensitive to the initial guess of Ra and σ_i. The effects of Reynolds number on the critical Rayleigh number, wave number and wave speed were investigated for values of Prandtl number ranging from 0.0001 to 1.0. Attention was focused on low Prandtl number fluids due to the importance of this range in materials processing applications involving liquid metals.

An interesting type of instability was found for a shallow cavity flow. The traveling wave neutral curve is shown in Figs. 3 and 4. The neutral curve has two minima. For example, at $Pr = 0.01$ and $Re = 700$ the first minima is at $k_1 = 1.45$ and the second minima at $k_1 = 5.1$, but for $Pr = 0.1$ and $Re = 300$ one minima is at $k_1 = 1.35$ and the other at $k_1 = 4.5$. Most of the results show two such minima as Pr or Re are increased. The flow becomes unstable at $k_1 = 1.35$ for $Pr = 0.01$ and for $Pr = 0.1$ at $k_1 = 4.5$. When the Reynolds number is increased, the two values of the minima shift their positions relative to one another in such a way that increasing the Reynolds number shifts the higher wave number minimum to lower Rayleigh numbers that determine the critical value. Similar results were obtained as the Prandtl number was increased. For example, at $Pr = 0.01$ the second minimum first appears at $Re = 300$, while for $Pr = 0.1$ it starts at $Re = 200$. Similarly, two minimum wave numbers were also found by others [26–28] for natural convection flow in a vertical slot. The lower value of the wave number minimum defines the instability of the flow when the buoyancy force predominates (i.e. thermal stability), while for larger Reynolds number the shear force defines the instability and the higher wave number of the two minima is the critical value. From Fig. 4, at $Re = 300$ both minima in the wave number are almost at the same Rayleigh number because the thermal and hydrodynamic forces are of the same order of magnitude ($Gr/Re^2 = 1.2$). For $Re \geqslant 400$ the value of $Gr/Re^2 \ll 1$, and the hydrodynamic force defines the stability of the flow. From Figs. 3 and 4, it is clear that increasing Reynolds number shifts the stability boundary in the direction of increasing Rayleigh number.

Figure 5 shows the variation of critical wave number with Re for different Prandtl numbers. For $Pr < 0.01$ the critical wave number decreases monotonically; however, it is expected that increasing the Reynolds number above 1000 will make the second minimum the dominant one. It is clear that at certain Reynolds numbers the value of k_c (critical) switches to a higher value as the hydrodynamic force dominates the instability, and the switch occurs sooner as Pr increases. For $Pr \geqslant 1$ the flow is defined by hydrodynamic stability (i.e. the shear force). Figure 6 shows the phase velocity vs the Rayleigh numbers for different Reynolds numbers. For $Re = 0$ the instability is in the form of stationary rolls. As the Reynolds number increases the rolls travel at a speed depending on Pr. For a wave number less than the critical value the velocity of the traveling rolls is a very weak function of the Rayleigh number. Increasing the wave number the velocity of the rolls become a strong func-

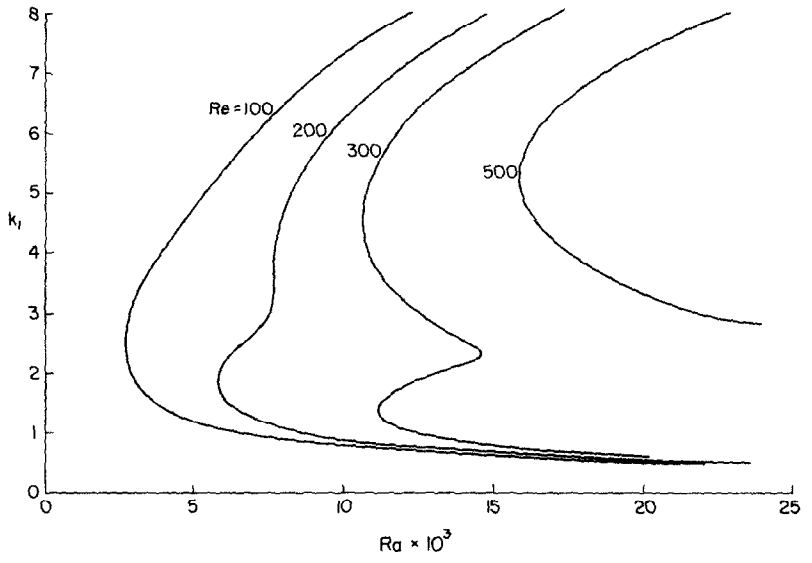

FIG. 4. Variation of wave number with Rayleigh number for different Reynolds numbers, $Pr = 0.1$, constant temperature boundary conditions.

tion of Ra, and for a certain value of Ra and k_l the velocity changes its sign. The critical value of the wave speed increases with an increase in the Reynolds number. The second tip which appears at $Re = 700$ and $Pr = 0.01$ at a wave speed of -100 is due to hydrodynamic stability.

Figure 7 and Table 2 shows how the critical Rayleigh number (Ra_c) varies with the Reynolds number for different Prandtl numbers. As the Reynolds and Prandtl numbers increase the critical Rayleigh number increases. Also, increasing Pr increases the critical value of Ra. For $Re = 0$ all the curves converge to the Benard solution ($Ra_c = 1707.76$).

Constant heat flux boundary condition

Figures 8–10 show the neutral Rayleigh number as a function of the wave number for a range of Reynolds numbers with $Pr = 0.01, 0.05, 0.1$ and 1, respectively. A second minimum is observed for $Re \geqslant 200$ and $Pr = 0.05$ (Fig. 9) and for $Re = 200$ and $Pr = 0.1$ (Fig. 10). This indicates an early appearance of the second minimum as the Prandtl number increases. While for $Pr = 1$ and $Re = 100$ (Fig. 10), the first minimum does not exist, and the trends are similar to those for the constant temperature boundary condition. In other words, the effect of the buoyancy force is not significant and stability is mainly due to

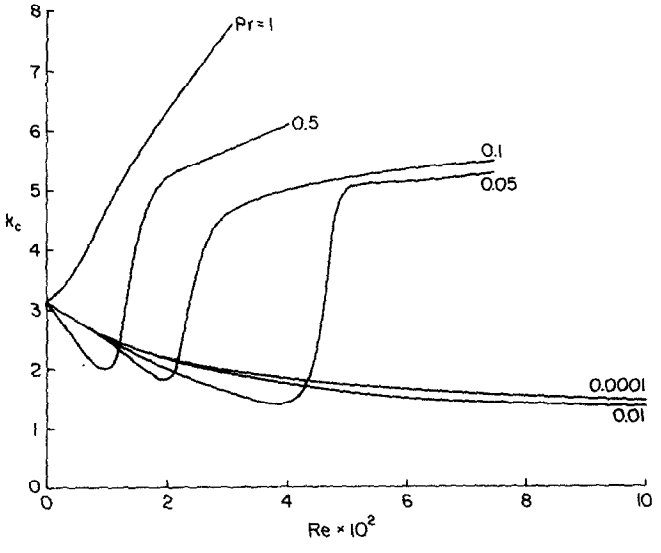

FIG. 5. Variation of the critical wave number with Reynolds number for different Prandtl numbers, constant temperature boundary conditions.

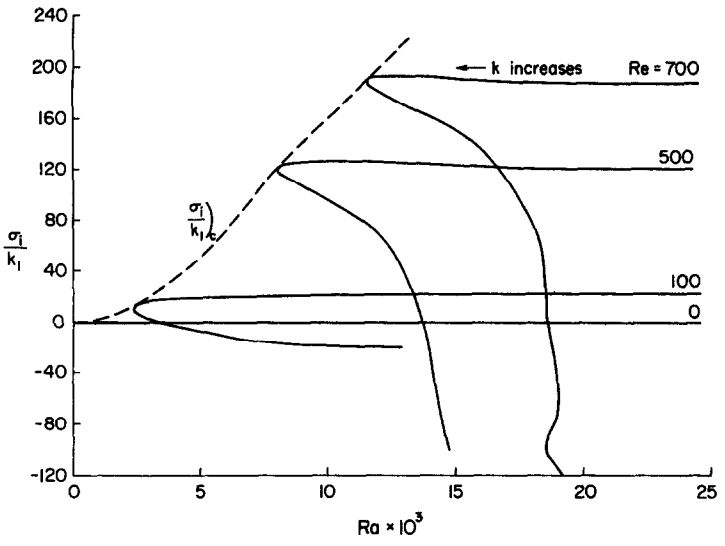

FIG. 6. Variation of the phase velocity with Rayleigh number for different Reynolds numbers, $Pr = 0.01$, constant temperature boundary conditions.

the shear force, while for $Pr \leqslant 0.1$ and the Reynolds number range investigated the stability is due to the buoyancy force. This is because the temperature fluctuation at the boundary has more freedom than for the constant temperature boundary condition. Amplification of the disturbance begins as $k \to 0$, i.e. very long wavelength. The value of the critical Rayleigh number increases with increasing Reynolds number. In addition, increasing the Reynolds number decreases the range of unstable wave numbers.

A sharp discontinuity was found for $Pr = 0.05$ and $Re = 300$ as well as for $Pr = 0.1$ and $Re = 200$ (Figs. 9 and 10). A discontinuity is not evident for the constant temperature boundary condition. To insure that the results are correct for such a range of parameters, the value of k_1 was increased by only 0.01 during the computations. More than 100 points were used to draw the portions of the curve near the discontinuity at $Re = 300$ and 200 in Figs. 9 and 10, respectively.

Figure 11 shows the variation of wave speed with the neutral Rayleigh number. The wave speed has different trends compared to those for the constant temperature boundary condition (Fig. 6). Increasing the Rayleigh number increases the speed of the traveling waves, which depends on the Reynolds number. The speed then decreases and changes its sign. For $Re = 300$ the wave speed of -35 is due to the shear effect (hydrodynamic stability). Also, Fig. 11 shows the wave speed asymptotically approaches a constant value as the Rayleigh number increases and the value depends on the Reynolds number.

Figure 12 and Table 3 shows the variation of the

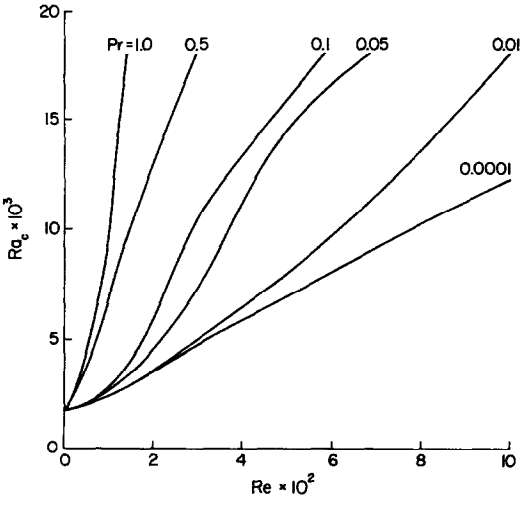

FIG. 7. Variation of the critical Rayleigh number with Reynolds number for different Prandtl numbers, constant temperature boundary conditions.

Table 2. Critical values of Rayleigh number, wave number and complex growth rate for constant temperature boundary conditions

Pr	Re	Ra_c	k_c	σ_i
0.01	100	2367.13	2.53	26.74
	200	3610.58	2.10	67.16
	500	7946.10	1.61	195.01
	700	11462.91	1.41	267.42
	1000	18048.13	1.18	353.47
0.05	100	2484.34	2.50	19.47
	200	4535.21	2.00	46.77
	300	7227.06	1.65	71.07
	400	11176.75	1.40	90.68
	500	14514.70	5.00	−465.53
	600	16636.47	5.15	−593.16
0.1	100	2749.75	2.50	12.95
	200	5843.99	1.80	31.97
	300	10678.91	4.60	−232.30
	500	15854.62	5.20	−529.69
	600	18587.92	5.38	−682.12
	700	21596.37	5.45	−821.06

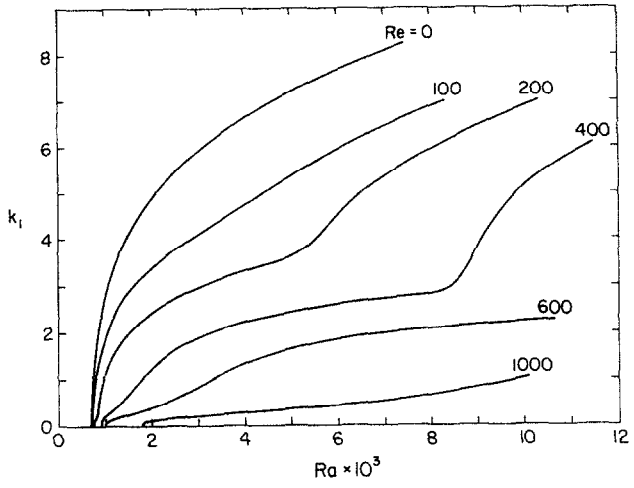

FIG. 8. Variation of wave number with the Rayleigh number for different Reynolds numbers, $Pr = 0.01$, constant heat flux boundary conditions.

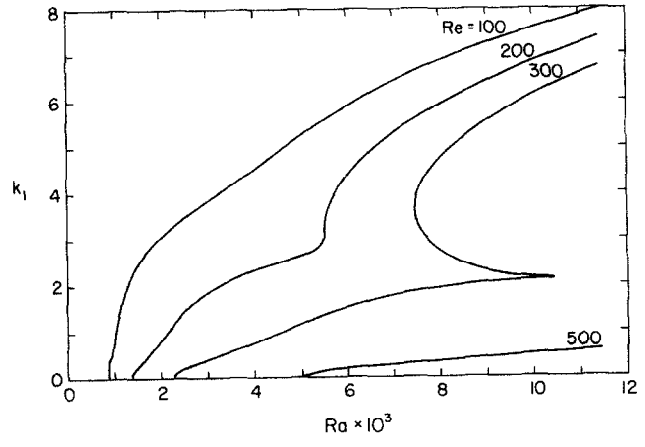

FIG. 9. Variation of wave number with the Rayleigh number for different Reynolds numbers, $Pr = 0.05$, constant heat flux boundary conditions.

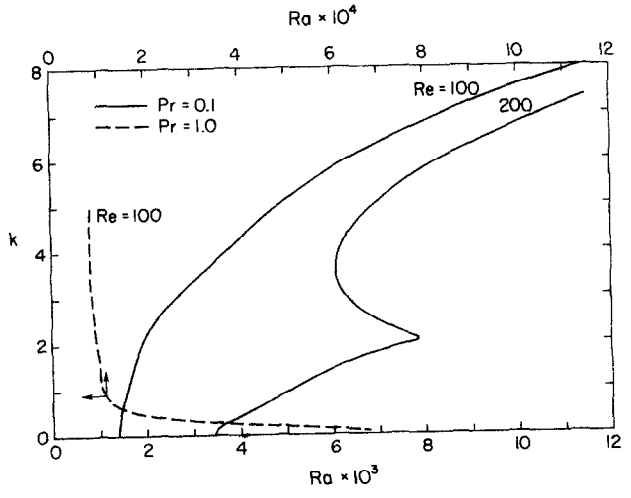

FIG. 10. Variation of wave number with the Rayleigh number for $Re = 100$ and 200 for $Pr = 0.1$ and 1.0, constant heat flux boundary conditions.

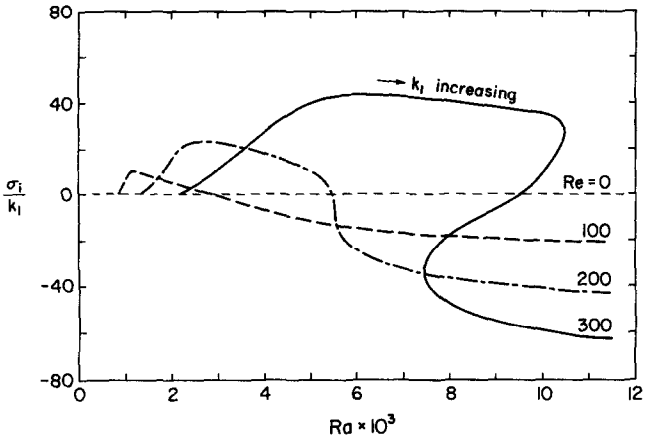

FIG. 11. Variation of the phase velocity with Rayleigh number for different Reynolds numbers, $Pr = 0.05$, constant heat flux boundary conditions.

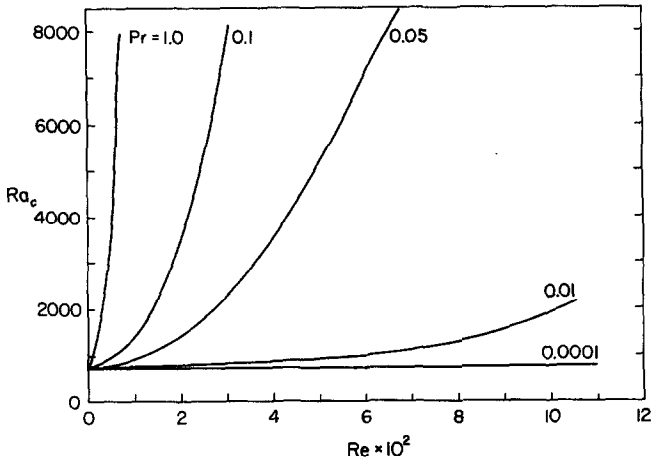

FIG. 12. Variation of the critical Rayleigh number with Reynolds number for different Prandtl numbers, constant heat flux boundary conditions.

Table 3. Critical values of Rayleigh number, wave number and complex growth rate for constant heat flux boundary conditions

Pr	Re	Ra_c	k_c	σ_i
0.01	100	729.79	0.01	0.00
	200	758.54	0.00	0.00
	400	878.54	0.00	0.00
	600	997.88	0.00	0.00
	1000	1882.31	0.00	0.00
0.05	100	892.27	0.00	0.00
	200	1410.50	0.00	0.00
	300	2279.96	0.00	0.00
	500	5109.93	0.00	0.00
0.1	100	1406.79	0.00	0.00
	200	3472.41	0.00	0.00
	400	11816.59	0.00	0.00
1.0	100	8295.50	400	−81.81

critical Rayleigh number with the Reynolds number for different Prandtl numbers. For $Pr = 0.0001$ the Rayleigh number is practically independent of the Reynolds number. For the range of Reynolds number investigated, increasing the Reynolds number stabilizes the flow for $Pr > 0$.

General boundary conditions

A Biot number of zero simulates a constant heat flux boundary condition, as discussed above. A Biot number approaching infinity simulates a constant temperature boundary condition. Experimentally it is difficult to achieve the above values (i.e. Biot number equal to zero or infinity), because it requires precise control of temperature or heat flux at the boundary. Hence, realistic values of the Biot number are between these two limits. Figure 13 shows the effect of con-

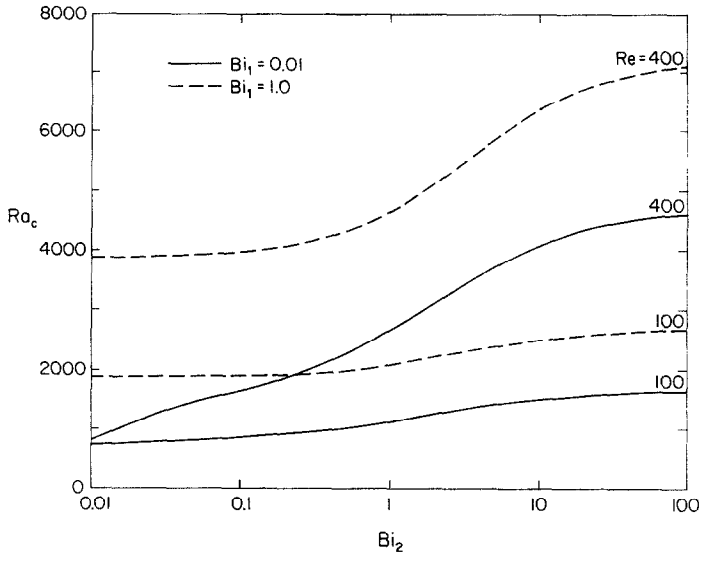

FIG. 13. Variation of the critical Rayleigh number with the upper boundary Biot number for different lower boundary Biot numbers and Reynolds numbers, $Pr = 0.01$.

vective boundary conditions on the critical Rayleigh number. For $Pr = 0.01$, increasing the Biot numbers raised the critical value of the Rayleigh number, since higher Biot numbers enhance the damping effect of the temperature at the boundaries.

CONCLUSIONS

The hydrodynamic and thermal stability of a flow field produced by combined thermal buoyancy and lid driven shear forces in a shallow cavity have been studied. The eigenvalue problem resulting from linear stability analysis has been solved by a numerical scheme general enough to handle a wide range of parameters such as Re, Pr and boundary conditions. Based on the results obtained the following conclusions can be drawn.

(1) Two minimum wave numbers appear in the shallow cavity flow, each describes a different kind of instability mechanism (thermal and hydrodynamic).

(2) For constant temperature boundary conditions the critical wave number switches from a lower value to a higher value due to a change in the relative magnitude of the driving forces. The smaller value corresponds to the buoyancy dominated flow and the higher value to the hydrodynamic forces dominated flow. This kind of switching is not predicted for a constant heat flux boundary condition. The stability is due primarily to the thermal effect for the case of a constant heat flux boundary condition, because the first derivative of the temperature disturbance is damped at the boundary instead of disturbance itself as in the case of the constant temperature boundary condition.

(3) Decreasing the Prandtl number of the fluid makes the flow more unstable.

(4) Increasing the Reynolds number stabilizes the flow for the values of parameters investigated. Also, increasing the Reynolds number decreases the width of unstable wave numbers.

(5) A stationary lid produces stationary rolls, while a moving lid produces traveling rolls. The speed of traveling cells is a function of controlling parameters.

REFERENCES

1. G. Z. Gershuni and E. M. Zhukhovitskii, *Convective Stability of Incompressible Fluid*. Izdatel'stvo Nauka, Moskva (1972).
2. P. G. Daniels, Roll-pattern evolution in finite-amplitude Rayleigh–Benard convection in a two-dimensional fluid layer bounded by distant sidewall, *J. Fluid Mech.* **143,** 125–152 (1984).
3. R. D. Benguria and M. C. Depassier, Oscillatory instabilities in the Rayleigh–Benard problem with a free surface, *Physics Fluids* **30,** 1678–1682 (1987).
4. J. N. Koster and U. Muller, Oscillatory convection in vertical slots, *J. Fluid Mech.* **139,** 363–390 (1984).
5. V. D. Murty, A study of the effect of aspect ratio on Benard convection, *Int. Commun. Heat Mass Transfer* **14,** 201–209 (1987).
6. K. Chandra, Instability of fluids heated from below. *Proc. R. Soc. London* **A164,** 231–242 (1938).
7. A. P. Gallagher and A. McD. Mercer, On the behavior of small disturbances in plane Couette flow with a temperature gradient, *Proc. R. Soc. London* **A286,** 117–128 (1965).
8. J. W. Deardorff, Gravitational instability between horizontal plates with shear, *Physics Fluids* **8,** 1027–1030 (1965).
9. K. S. Gage and W. H. Reid, The stability of thermally stratified plane Poisseuille flow, *J. Fluid Mech.* **33,** 21–32 (1968).
10. G. J. Hwang and K. C. Cheng, Convection instability in the thermal entrance region of a horizontal parallel-plate channel heated from below, *J. Heat Transfer* **95,** 72–77 (1973).
11. G. Vanderbroch and J. K. Platten, Approximate (variational) and exact (numerical) solutions of Benard type

problems with temperature dependent material properties, *Int. J. Engng Sci.* **12,** 897–917 (1974).
12. Y. Kamotani, S. Ostrach and H. Miao, Convective heat transfer augmentation in thermal entrance regions by means of thermal instability, *J. Heat Transfer* **101,** 222–226 (1979).
13. R. C. Di Prima and J. T. Stuart, Hydrodynamic stability, *J. Appl. Mech.* **50,** 983–991 (1983).
14. B. J. Bayly, S. A. Orszag and T. Herbert, Instability mechanisms in shear-flow transition, *Ann. Rev. Fluid Mech.* **20,** 359–392 (1988).
15. J. K. Platten and J. C. Legros, *Convection in Liquids.* Springer, New York (1984).
16. L. A. B. Pilkington, Review lecture: the float glass process, *Proc. R. Soc. London* **A314,** 1–25 (1969).
17. M. G. Veladre, *Natural Convection,* von Karman Institute of Fluid Dynamics, Lecture Series 1980-7 (1980).
18. J. Hart, A note on the stability of low Prandtl number Hadley circulations, *J. Fluid Mech.* **132,** 271–281 (1983).
19. B.A. Finlayson, The Galerkin method applied to convective instability problems, *J. Fluid Mech.* **33,** 201–208 (1968).
20. H. P. Kuo, S. A. Korpela, A. Chait and P. S. Marcus, Stability of natural convection in a shallow cavity. In *Heat Transfer* (Edited by C. L. Tien, V. P. Carey and J. K. Farrell), Vol. 4, pp. 1539–1544. Hemisphere, Washington, DC (1986).
21. H. P. Kuo and S. A. Korpela, Stability and finite amplitude natural convection in a shallow cavity with insulated top and bottom and heated from a side, *Physics Fluids* **31,** 33–42 (1988).
22. V. U. K. Sastry and K. V. R. Rau, Numerical solution of the stability of hydrodynamic Couette flow with wall currents, *Int. J. Engng Sci.* **15,** 405–412 (1977).
23. D. P. Chock and C. H. Li, Direct integration method applies to Soret-driven instability, *Physics Fluids* **18,** 1401–1406 (1975).
24. A. Davey, On the stability of plane Couette flow to infinitesimal disturbances, *J. Fluid Mech.* **57,** 369–380 (1973).
25. S. A. Orszay, Accurate solution of the Orr–Sommerfeld stability equation, *J. Fluid Mech.* **50,** 689–703 (1971).
26. A. F. Gill and A. Davey, Instabilities of a buoyancy-driven system, *J. Fluid Mech.* **75,** 775–793 (1969).
27. R. F. Bergholz, Instability of steady natural convection in a vertical fluid layer, *J. Fluid Mech.* **84,** 743–768 (1978).
28. M. N. Ozisik, Thermal stability of a vertical fluid layer with volumetric energy sources. In *Natural Convection Fundamentals and Applications* (Edited by S. Kakac, W. Aung and R. Viskanta), pp. 156–178. Hemisphere, Washington, DC (1985).

STABILITE DANS UNE CAVITE PEU PROFONDE A COUVERCLE MOBILE ET CHAUFFEE PAR LE BAS

Résumé—La stabilité hydrodynamique et thermique d'un écoulement cisaillant flottant thermiquement dans une cavité peu profonde est analysée par la théorie linéarisée de perturbation. On considère une cavité chauffée par dessous et refroidie sur le couvercle mobile. Une procédure numérique qui est générale vis-à-vis des conditions aux limites, des nombres de Reynolds et de Prandtl, est décrite pour résoudre les équations du modèle linéarisé. Une intégration directe numérique (Runge–Kutta avec Newton–Raphson) est utilisée pour résoudre les équations aux dérivées partielles du bilan. Cette méthode donne un résultat exact pour le problème classique de Bénard avec apparition d'instabilité au nombre de Rayleigh critique $Ra_c = 1707{,}76$. Les résultats numériques montrent l'existence de deux nombres d'onde critiques suivant que la force dominante qui gouverne l'écoulement est l'effet d'Archimède ou le cisaillement. Pour $Pr \leqslant 0{,}1$ l'instabilité est due à la force de flottement pour des conditions aux limites de flux thermique constant, tandis que pour $Pr = 1$ l'instabilité est due à la force de cisaillement. Un accroissement du nombre de Reynolds stabilise l'écoulement et une réduction du nombre de Prandtl rend l'écoulement plus instable.

STABILITÄT VON SCHERSTRÖMUNGEN IN EINEM FLACHEN, VON UNTEN BEHEIZTEN HOHLRAUM

Zusammenfassung—Es wird die hydrodynamische und thermische Stabilität einer kombinierten Auftriebs- und (horizontalen) Scherströmung in einem flachen Hohlraum mit Hilfe der linearisierten Störungstheorie untersucht. Der Hohlkörper wird von unten beheizt und an der oberen, sich bewegenden Abdeckung gekühlt. Es wird ein numerisches Verfahren zur Lösung der linearisierten Modellgleichungen beschrieben, das im Hinblick auf die Randbedingungen sowie die Reynolds- und Prandtl-Zahl allgemeingültig ist. Die auftretenden Differentialgleichungen werden mit Hilfe eines direkten numerischen Integrationsverfahrens (Runge–Kutta mit Newton–Raphson) gelöst. Man erhält eine exakte Lösung für das klassische Benard-Problem, bei dem die Strömung bei einer kritischen Rayleigh-Zahl von $Ra_c = 1707{,}76$ instabil wird. Anhand der numerischen Ergebnisse können 2 kritische Wellen-Zahlen festgestellt werden, je nachdem, ob die Antriebskräfte der Strömung durch Auftrieb oder Scherung dominiert werden. Für $Pr \leqslant 0{,}1$ wird die Instabilität durch die Auftriebskraft, bei konstanter Wärmestromdichte als Randbedingung, verursacht, während bei $Pr = 1$ die Scherkräfte für die Instabilität verantwortlich sind. Mit zunehmender Reynolds-Zahl stabilisiert sich die Strömung, durch Reduzierung der Prandtl-Zahl können instabilere Strömungsverhältnisse erzeugt werden.

УСТОЙЧИВОСТЬ ТЕЧЕНИЯ В НАГРЕВАЕМОЙ СНИЗУ НЕГЛУБОКОЙ ПОЛОСТИ СО СЪЕМНОЙ КРЫШКОЙ

Аннотация—На основе линеаризованной теории возмущений анализируется гидродинамическая и термическая устойчивость тепловой свободной конвекции и течения с поперечным градиентом скорости в неглубокой полости. Рассматривается полость, нагреваемая снизу и охлаждаемая у верхней движущейся крышки. Описывается методика численного решения линеаризованных модельных уравнений, обобщенная для различных граничных условий, а также чисел Рейнольдса и Прандтля. При решении дифференциальных уравнений сохранения используется прямой метод численного интегрирования (Рунге–Кутта и Ньютона–Рафсона). Данный метод позволяет получить точный результат для классической задачи Бенара, в которой течение становится неустойчивым при критическом числе Рэлея, равном $Ra_c = 1707{,}76$. Численные результаты указывают на существование двух критических волновых чисел в зависимости от того, чем вызывается течение—подъемной силой или сдвигом. В случае $Pr \leqslant 0{,}1$ неустойчивость индуцируется подъемной силой при граничных условиях с постоянным тепловым потоком, в то время как при $Pr = 1$ она обусловлена сдвигом. При увеличении значения числа Рейнольдса течение стабилизируется, а при уменьшении значения числа Прандтля оно становится более неустойчивым.